

Expression of MLN64 influences cellular matrix adhesion of breast cancer cells, the role for focal adhesion kinase

WEI CAI^{1,2}, LIN YE¹, JIABANG SUN², ROBERT E. MANSEL¹ and WEN G. JIANG¹

¹Metastasis and Angiogenesis Research Group, Department of Surgery, Cardiff University School of Medicine, Heath Park, Cardiff CF14 4XN, UK; ²Department of General Surgery, XuanWu Hospital, Capital Medical University, Beijing, P.R. China

Received December 11, 2009; Accepted January 11, 2010

DOI: 10.3892/ijmm_00000379

Abstract. The *metastatic lymph node 64 (MLN64)* gene was initially identified as highly expressed in the metastatic lymph node from breast cancer. It is localized in q12-q21 of the human chromosome 17 and is often co-amplified with *erbB-2*. However, the role played by MLN64 in breast cancer remains unclear. In the present study, the expression of MLN64 was examined in a breast cancer cohort using quantitative real-time PCR and immunohistochemical staining. It demonstrated that MLN64 was highly expressed in breast tumours compared to corresponding background tissues at both transcript level and protein level. The elevated level of MLN64 transcripts was correlated with the poor prognosis and overall survival of the patients. A panel of breast cancer cell sublines was subsequently developed by knockdown of MLN64 expression. Loss of MLN64 expression in MCF-7 cells resulted in a significant reduction of cell growth (absorbance for MCF-7^{ΔMLN64} being 0.87±0.07, P<0.01 vs. wild-type control (MCF-7^{WT} 1.13±0.06) and transfection control (MCF-7^{PEF} 1.27±0.05). In cell-matrix adhesion assay, MDA-MB-231^{ΔMLN64} cells showed a significant increase in adhesion (86±14), p<0.01 compared with both MDA-MB-231^{WT} (61±20) and MDA-MB-231^{PEF} (45±27). Further investigations demonstrated an increase in protein level of the focal adhesion kinase (FAK) in MDA-MB-231^{ΔMLN64} cells using Western blot analysis and immunofluorescent staining of FAK. Moreover, addition of FAK inhibitor to these cells diminished the effect of MLN64 on cell-matrix adhesion, suggesting that FAK contributed to the increased adhesion in MDA-MB-231^{ΔMLN64} cells. In conclusion, MLN64 is overexpressed in breast cancer, and its level correlates with poor prognosis and patient survival. MLN64 contributes to the development and progression of breast cancer through the regulation of cell proliferation and adhesive capacity.

Introduction

Breast cancer is the most common cancer in women in Europe and North America affecting up to one in eight women over their lifetime (1). Despite recent advances made in diagnosis and treatment, breast cancer remains the leading cause of cancer-related mortality in women.

MLN64 (metastatic lymph node 64), which was initially identified from a breast cancer-derived metastatic lymph node cDNA library, has been localized to the q12-q21 of the long arm of chromosome 17 (2). *MLN64* gene encodes a 445 amino-residue protein containing two distinct domains. Its N-terminus consists of a MENTAL (*MLN64* N-Terminal) domain similar to *MLN64* N-terminal homologue (*MENTHO*), containing four potential transmembrane regions and target the protein to the membrane of late endosome (3). By immunocytofluorescent staining, *MLN64* protein was observed to be localized within bundle-like structures distributed throughout the cell cytoplasm and condensed in a perinuclear patch. If its N-terminus was removed, *MLN64* was homogeneously distributed in the cytoplasm, suggesting that N-terminus acts on the specific cytoplasmic localization of *MLN64* (4). Its C-terminus contains a StAR-related transfer domain (*START*) that is highly homologous to steroidogenic acute regulatory protein (*StAR*) (4). *StAR* is a mitochondrial protein involved in the acute synthesis of steroids in adrenal and gonad (5). Homology between these molecules further raises the possibility that *MLN64* has steroidogenic activity. X-ray crystallography indicates that the *START* domain, like *StAR* protein, forms a hydrophobic tunnel structure that can bind a single cholesterol molecule (6-8). Recent evidence suggests that *MLN64* plays a key role in steroidogenesis by enhancing the cholesterol transport at the surface of late endosome (2,4,9,10). Moreover, *MLN64* has been proposed to mediate *StAR*-independent steroidogenesis, because *MLN64* mRNA was detected in some tissues, such as placenta and brain, which produce steroid hormones but do not express *StAR* (10).

Amplification of certain region in chromosome 17q has been indicated in various solid tumours, including breast cancer, prostate cancer and upper gastrointestinal adenocarcinomas (2,11,12). This region encodes various genes which play critical roles in carcinogenesis and disease progression, such as *ERBB2*, *GRB7* (growth factor receptor-bound protein 7) and

Correspondence to: Professor Wen G. Jiang, Metastasis and Angiogenesis Research Group, Department of Surgery, Cardiff University School of Medicine, Heath Park, Cardiff CF14 4XN, UK
E-mail: jiangw@cf.ac.uk

Key words: MLN64, adhesion, breast cancer

MLN64. The amplification can be observed in 20-30% breast cancers within the region of chromosome 17q12, containing *MLN64* gene (1). *MLN64* is highly expressed in certain breast carcinomas, often co-amplified with *erbB-2*, and thus may contribute to the development and progression of breast tumours by mediating the intratumoral steroidogenesis (2,13-15). The elevated expression of *MLN64* has also been demonstrated in prostate cancer which is co-expressed with *CYP-17*. *CYP-17* encodes a key enzyme in androgen synthesis (12).

Although overexpression of *MLN64* has been indicated in certain solid tumours, its biological function in tumour cells and how it is involved in the disease progression remain largely unknown. In the present study, we investigated the functional aspect of *MLN64* in breast cancer cells after creating sublines of breast cancer cells in which *MLN64* was knocked down using specific ribozyme transgenes. The expression of *MLN64* was also examined in a breast cancer cohort, and analysed against the clinical aspects.

Materials and methods

Cell lines and cells culture. Human breast cancer cell lines, MDA-MB-231 and MCF-7 were obtained from the European Collection of Animal Cell Cultures (ECACC, Salisbury, England). Cells were routinely cultured with Dulbecco's modified Eagle's medium containing 10% fetal calf serum, 100 U/ml penicillin and 100 µg/ml streptomycin at 37°C and 5% carbon dioxide.

Human breast specimens. A total of 146 breast samples were collected immediately after surgery and stored at -80°C until use, with approval of the local ethics committee. It included 113 breast cancer tissue and 33 background normal breast tissues which were from the same patients. All the specimens used in the current study were verified by a consultant pathologist. Patients were routinely followed clinically after surgery and details were stored in a database. The median follow-up period was 120 months. The clinical data are provided in Table I.

Immunohistochemical staining of *MLN64*. Frozen specimens of mammary tissues were cut at a thickness of 6 µm using a cryostat (Leica CM 1900, Leica Microsystems UK Ltd., Buckinghamshire, UK). The sections were mounted on super frost plus microscope slides, air dried and then fixed in the mixture of 50% acetone and 50% methanol for 15 min. After 10-min air-drying, the slides were placed into OptiMax Wash Buffer (BioGenex, San Ramon, USA) for 5 min to rehydrate. The slides were incubated for 20 min in a blocking solution that contained 10% horse serum and probed with anti-*MLN64* antibody (Santa Cruz Biotechnology) for 1 h. Following extensive washing, the slides were incubated for 30 min with a biotinylated secondary antibody (Multilink swine anti-goat/mouse/rabbit immunoglobulin, Dako Inc. Carpinteria, CA). After washing, slides were placed in avidin-biotin complex (ABC-Vector Labs) for 30 min. Diaminobenzidine chromogen (Vector Labs) was then added to the slides and incubated in the dark for 5 min. The slides were counterstained with Mayer's haematoxylin for 1 min and dehydrated in

ascending grades of ethanol before clearing in xylene and mounting under a cover slip.

Reverse transcription-PCR. Total RNA extraction from frozen tissues and culture cells was performed using Total RNA Isolation Reagent (ABgene, Epsom, UK). The concentration of RNA was determined using an ultraviolet spectrophotometer. Routine RT-PCR was carried out using a PCR master mix that was commercially available (AbGene), then run in a GeneAmp PCR System 2400 thermocycler (Perkin-Elmer). The sequences of primers used were: *MLN64*: 5'-GC ACCTTTGTCTGGATTCTT-3' and 5'-TGAAAGGCAAAT TCAAACAT-3'.

Reactions were carried out at the following conditions: 94°C for 5 min, 35 cycles of 94°C for 30 sec, 55°C for 30 sec and 72°C for 30 sec, followed by a final extension of 5 min at 72°C. PCR products were separated on a 2% agarose gel and photographed using a digital camera mounted over a UV transilluminator after a staining with ethidium bromide. The quality of cDNA was verified using *GAPDH* primers (5'-AGC TTGTCATCAATGGAAAT-3' and 5'-CTTACCACCTTC TTGATGT-3').

Real-time quantitative PCR. The level of *MLN64* transcripts from the prepared cDNA was determined using a real-time quantitative PCR, based on Amplifluor technology, modified from a method reported previously (16). An additional sequence was added to one of the primers, known as the Z sequence (5'-actgaacctgacctgaca-3') which is complementary to the universal Z probe (Intergen Inc., Oxford, UK). The reaction was carried out on IcylerIQ™ (Bio-Rad, Hemel Hemstead, UK) which is equipped with an optic unit that allows real-time detection of 96 reactions. The reaction condition was: 94°C for 12 min, 50 cycles of 94°C for 15 sec, 55°C for 40 sec (the data capture step) and 72°C for 20 sec. The levels of the transcripts were generated from an internal standard that was simultaneously amplified with the samples.

Construction of ribozyme transgene targeting human *MLN64* and the establishment of corresponding stable transfectants. Anti-human *MLN64* hammerhead ribozymes were designed based on the secondary structure of the gene generated using the Zuker RNA mFold program (17). The ribozymes were accordingly synthesized and then cloned into pEF6/V5-His TOPO vector (Invitrogen, Paisley, UK). The verified ribozyme transgenes and empty plasmids were transfected into MDA-MB-231 and MCF-7 cells respectively using an Easyjet Plus electroporator (EquiBio, Kent, UK). After up to 14 days of selection with 5 µg/ml blasticidin, the verified transfectants were cultured in maintenance medium containing 0.5 µg/ml blasticidin. Primer sequences of the ribozymes were 5'-CTG CAGGTGCGAGGAGAGGCTCTGGCTGTGGCTGATGA GTCCGTGAGGA-3' and 5'-ACTAGTGGCCTCCCTGGTC CTCCTGTTTCGTCCTCACGGACT-3'.

Cell growth assay (18). Breast cancer cells were plated into 96-well plates at 3,000 cells/well. Cells were fixed in 4% formaldehyde on the day of 1, 3, 5 after plating. The cells were then stained with 0.5% (w/v) crystal violet. Following washing, stained crystal violet was extracted with 10% (v/v) acetic

acid. Absorbance was determined at a wavelength of 540 nm using an ELx800 spectrophotometer.

Flow cytometric analysis of apoptosis (19). All cells including those floating in the culture medium were harvested after a period of incubation. Cells were washed in cold PBS and resuspended in 1X annexin-binding buffer at a density of 1×10^6 cells/ml after centrifugation. FITC annexin V (5 μ l) and 1 μ l of the PI working solution (100 μ g/ml) (Molecular Probes, Oregon, USA) were added to 100 μ l of the cell suspension. After a 15 min incubation at room temperature, 400 μ l of 1X annexin-binding buffer was added, mixed gently and the samples were kept on ice. The stained cells were immediately analyzed using the flow cytometer and FlowMax software package.

Cell matrix adhesion. Cells (30,000) were added to each well of a 96-well plate which was pre-coated with Matrigel (5 μ g/well) (BD Biosciences, Oxford, UK). After 40 min of incubation, non-adherent cells were washed off using BSS buffer. The remaining cells were fixed with formalin and stained with crystal violet. The number of adherent cells was then counted. When the effect of FAK on adhesion was studied, 10 nM FAK inhibitor (PF573228, Tocris, Bristol, UK) was added in the corresponding wells.

In vitro invasion assay. This was performed as previously reported and modified in our laboratory (20). Briefly, transwell inserts (upper chamber) with 8 μ m pores were coated with 50 μ g/insert of Matrigel and air-dried, before being rehydrated. Cells (30,000) were seeded into each well. After 72 h, cells that had migrated through the matrix and adhered on the other side of the insert were fixed and stained with crystal violet. The crystal violet was extracted with 10% (v/v) of acetic acid and the absorbance was obtained using a spectrophotometer.

In vitro motility assay using cytodex-2 beads. This was based on a method reported previously (20). Cells (1×10^6) were incubated with 100 μ l cytodex-2 beads (Pharmacia, Piscataway, NJ) in 10 ml DMEM overnight. After washing, the beads with adhered cells were resuspended in 1 ml of DMEM. Cell suspension (100 μ l) were transferred into each well of a 24-well plate. After 4 h of incubation, the beads were washed off using BSS. The migrated cells were then fixed and stained with crystal violet for counting.

In vitro migration/wounding assay. Cells were seeded into a 24-well plate and allowed to reach confluence. The cell monolayer was scraped using a fine gauge needle to create a wound of approximately 200 mm wide (21). The migration of cells to close the wound was then recorded and examined microscopically (Leitz DMIRB) on a heated stage using a time-lapse video recording facility. Images of wound closure between the two leading cell fronts were subsequently obtained at 30 min intervals and analyzed using an image analysis software Optimas (Version 6, Optimas, UK).

Electric cell-substrate impedance sensing (ECIS) based cellular adhesion assay. The 9600 model of the ECIS

instrument (Applied Biophysics Inc., NJ, USA) were used for adhesion assay in the study, as previously reported (22-24). The 8W10E arrays (8 wells, 10 electrodes in each well) were used in the present study. Following a pretreatment with L-cysteine solution, the arrays were incubated with the medium for 1 h. MDA-MB-231^{wt}, MDA-MB-231^{DEF}, MDA-MB-231^{MLN64} cells were seeded at 300,000 per well in 400 μ l medium. The impedance at 30 kHz was recorded for 2.5 h and the data was analysed using ECIS-9600 system.

Immunofluorescence staining of paxillin and FAK. Cells were seeded on chamber slides (NuncTM) at 20,000 cells per well. After 60 min of incubation, the cells were fixed in ice-cold ethanol for 20 min and then rehydrated with BSS buffer and permeabilized before staining. Anti-paxillin or anti-FAK antibody (BD Biosciences Pharmingen) was added and incubated for 1 h. Then specific FITC labelled secondary antibody (Dako, Glostrup, Denmark) was used to react in the dark for 1 h. Fluorescent staining was visualized using an OlympusTM BX51 microscope and imaged using a cooled C4742-80 digital camera (Hamamatsu Photonics UK, Welwyn Garden City, UK).

Western blot analysis of MLN64 and FAK. Cells were collected and lysed in HCMF buffer (25). The protein concentration was quantified using DC Protein Assay kit (Bio-RadTM) and an ELx800 spectrophotometer (Bio-Tek[®]). Equal amounts of protein from each sample (20 μ g/lane) were added onto a 10% sodium dodecyl sulfate-polyacrylamide gel. After electrophoresis, proteins were blotted onto nitrocellulose sheet and blocked in 10% skimmed milk for 60 min. Proteins were probed with the anti-human MLN64 and FAK antibody and the corresponding peroxidase-conjugated secondary antibodies. A molecular weight marker (SDS-6H; Sigma Chemical Co.) was used to determine the protein size. Protein bands were visualized with a Super-signalTM West Dura system and documented using a gel documentation system (UVITech, Cambridge, UK).

Statistical analysis. Statistical analysis was performed using SPSS. Mann-Whitney U-test was used for analysis of non-normally distributed data, while t-test was used for normally distributed. Survival was analyzed using Kaplan-Meier survival analysis. $P < 0.05$ was considered statistically significant.

Results

The expression of MLN64 was examined in a variety of breast cancer cells using RT-PCR. Higher level of transcript expression was seen in breast cancer cells and the breast cancer tissue, compared with the normal mammary background tissue (Fig. 1B). Interestingly, we found that in some normal human cell lines (HECV, MRC-5) MLN64 transcripts were also detectable. Similar result was found in the real-time quantitative PCR (Fig. 1C). Breast cancer tissue had higher level of transcripts (median 1.08 copies) compared with normal mammary tissues (median 0.50 copies), but the difference was not statistically significant ($P=0.13$).

Immunohistochemical staining of MLN64 protein was observed in the human breast tissue section ($n=32$ pairs).

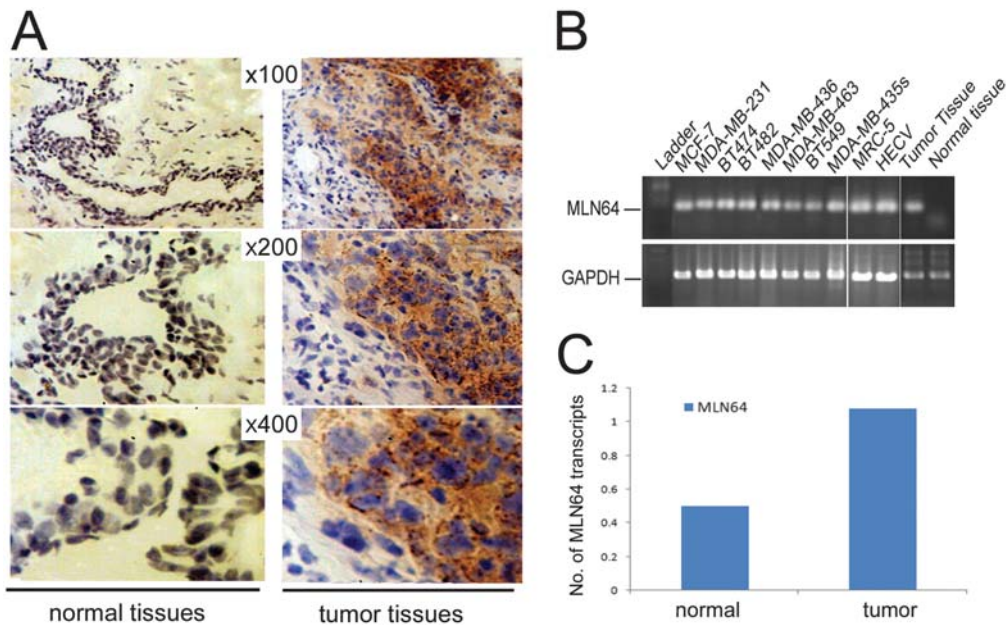


Figure 1. MLN64 expression in breast cancer tissue and cell lines. (A) Immunohistochemical staining of MLN64 in normal mammary tissues (left panel) and tumour tissues (right panel) with different magnifications in the same region. (B) Detection of the MLN64 transcripts in different cell lines and breast tissue specimens using RT-PCR. GAPDH was used as the housekeeping control. (C) Quantitative analysis of MLN64 transcripts in normal and tumour tissues with Q-PCR.

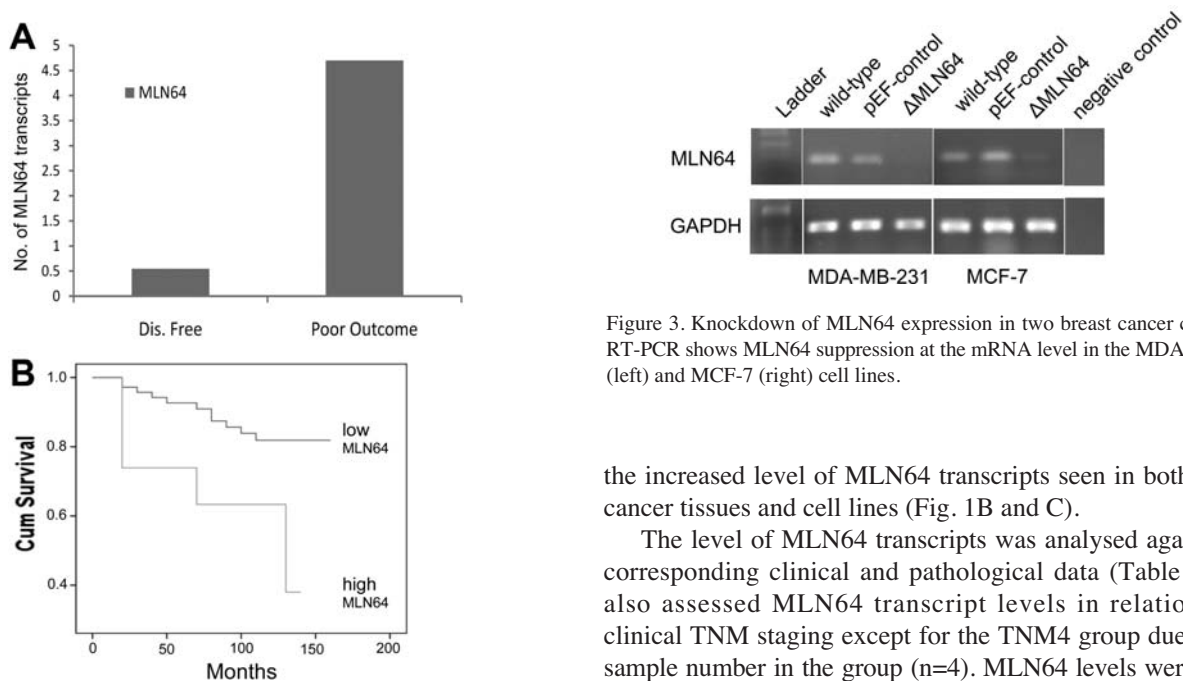


Figure 2. MLN64 expression and clinical outcome and long-term survival. (A) Expression level of MLN64 and clinical outcome. The MLN64 transcripts levels in patients disease-free are lower than those patients who had poor outcome ($p=0.001$), including local recurrence, metastases and died of breast cancer. (B) Kaplan-Meier survival curves: the overall survival of patients who had lower level of MLN64 transcripts was better than those patients with higher expression ($p=0.012$).

MLN64 protein was detected to be strongly stained in the cytoplasm of breast cancer cells in the specimen, while in the adjacent normal breast tissues, only little staining was seen (Fig. 1A). This pattern is consistent with the observation with

Figure 3. Knockdown of MLN64 expression in two breast cancer cell lines. RT-PCR shows MLN64 suppression at the mRNA level in the MDA-MB-231 (left) and MCF-7 (right) cell lines.

the increased level of MLN64 transcripts seen in both breast cancer tissues and cell lines (Fig. 1B and C).

The level of MLN64 transcripts was analysed against the corresponding clinical and pathological data (Table I). We also assessed MLN64 transcript levels in relation with clinical TNM staging except for the TNM4 group due to low sample number in the group ($n=4$). MLN64 levels were lower in tumours of early stage (TNM1, median, 0.61 copies), and were increased in the tumours of the advanced P=0.018 and 0.015, compared with TNM2 (median, 2.56 copies) and TNM3 (median, 4.09 copies), respectively. Therefore, MLN64 expression was correlated with tumour spread. The relationship between the levels of MLN64 transcripts and histological types and nodal status were also analysed (Table I). Tumours with lymphatic involvement had higher levels of MLN64 transcripts than the node negative tumours. Although there was some elevated expression of MLN64 seen in the poorly differentiated tumours, but the differences were not statistically significant when compared with well differentiated and moderately differentiated tumours.

Table I. Breast cancer patients clinical data details and MLN64 transcript levels.

Clinical/pathological features	Sample no.	Median (copy no.)	IQR	P-value
Grade				
1	20	2.07	0.28-3.26	
2	39	1.00	0.19-4.70	0.614
3	52	0.87	0.19-7.37	0.758
NPI				
1 (<3.5)	59	0.83	0.16-3.89	
2 (3.5-5.4)	35	1.30	0.27-3.74	0.309
3 (>5.4)	15	1.20	0.2-11.0	0.248
TNM				
1	61	0.61	0.17-2.72	
2	36	2.56	0.21-11.3	0.018
3	7	4.09	1.14-27.5	0.015
4	4	0	0-302	
Clinical outcome				
Disease-free	81	0.55	0.15-2.86	
Poor outcome				
With metastasis	5			
With local recurrence	4	4.70	1.2-12.6	0.0001
Died of breast cancer	16			
Histology				
Ductal	89	1.01	0.19-4.44	0.396
Lobular	11	1.18	0.54-6.28	
Others	6	2.90	1.56-6.53	
Lymph node status				
Negative	59	0.83	0.16-3.89	0.28
Positive	50	1.24	0.25-6.30	

Using the Nottingham Prognostic Index, we further analysed the relationship between prognosis and MLN64 expression (Table I). Patients with moderate prognosis (NPI 3.4-5.4, median 1.30 copies) and poor prognosis (NPI >5.4, median 1.20 copies) exhibited higher levels, $p=0.309$ and $p=0.248$ when compared to the good prognosis [(NPI<3.4) patients (median 0.83 copies), respectively)]. Using clinical outcomes over the 10 year follow-up period, MLN64 was found to be elevated in those with poor outcomes including local recurrence, metastasis or died of breast cancer (median 4.70), $p=0.0001$ compared with those who were disease-free (median 0.55).

To investigate whether MLN64 expression levels were correlated with the long-term survival, we divided the patients into two groups according to their MLN64 transcript levels. Kaplan-Meier survival analysis demonstrated that patients with higher level of MLN64 transcripts had shorter overall survival (Fig. 2). The average overall survival of patients with higher MLN64 expression was 89.3 months (95% confidence interval 58.3-120.3 months), $p=0.012$, in comparison with 138.9 months in patients with lower

expression level (95% confidence interval 129.3-148.4 months).

The expression of MLN64 was knocked down using ribozyme transgenes targeting human MLN64 mRNA. This was performed in two breast cancer cell types, MCF-7 and MDA-MB-231, which expressed MLN64 (Fig. 1) The knockdown of MLN64 was verified in the transfectants using RT-PCR (Fig. 3). Marked reduction of MLN64 expression was seen in both MDA-MB231^{ΔMLN64} and MCF-7^{ΔMLN64} cells which were transfected with ribozyme transgenes, compared to their corresponding controls including wild-type and empty plasmid controls.

The effect of knocking down MLN64 on *in vitro* cell functions were examined including cell growth, adhesion, invasion, motility and migration. Loss of MLN64 in MDA-MB-231 cells had a significant impact on cell matrix adhesion (Fig. 4A). The MDA-MB-231^{ΔMLN64} cells exhibited a significantly stronger adhesion ability (adherent cell number 86±14), $p<0.01$ compared with both MDA-MB-231^{WT} (56±17) and MDA-MB-231^{pEF} cells (45±29). However, this effect was not seen in MCF-7^{ΔMLN64} cells (data not shown). Moreover, in

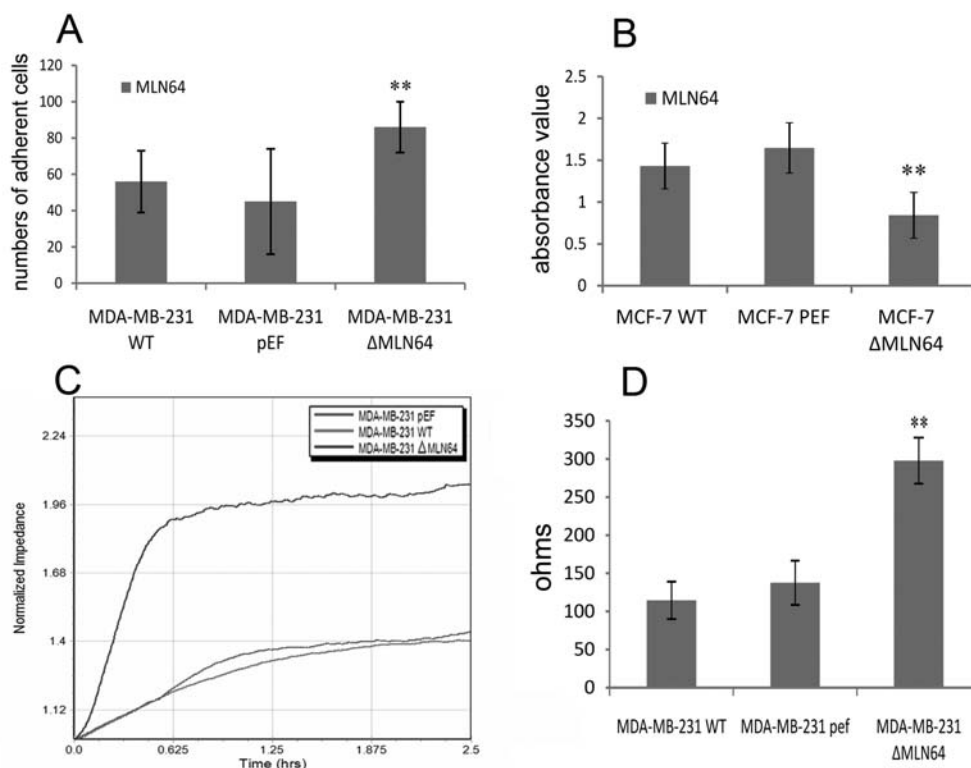


Figure 4. Influences on cell function by knockdown of MLN64 in breast cancer cells. (A) Adhesion in MDA-MB-231 cells. MDA-MB-231 Δ MLN64 cells exhibited the enhanced adhesiveness. (B) Cell growth in MCF-7 cells. MCF-7 Δ MLN64 cells had a reduction in cell growth. ** $p < 0.01$. (C) MLN64 knocked down on cell adhesion as analysed by ECIS. In the MDA-MB-231 cells which were knocked down MLN64 showed a markedly increased adhesion. (D) A significant increase of adhesion in MDA-MB-231 Δ MLN64 cells shown as the resistance at 2.5 h using ECIS, $n = 6$, ** $p < 0.01$ vs. MDA-MB231^{WT} and MDA-MB231^{pEF} controls.

migration, motility and invasion assays, knockdown of MLN64 in the cell lines did not show any obvious difference in comparison with the corresponding controls (data not shown).

In contrast, knockdown of MLN64 reduced the *in vitro* growth of MCF-7 cells, but not in the MDA-MB-231 cells (Fig. 4B). The absorbance of MCF-7 Δ MLN64 at day 5 was 0.84 ± 0.27 , $p < 0.01$ compared to MCF-7^{WT} cells (1.43 ± 0.26) and MCF-7^{pEF} cells (1.65 ± 0.29), respectively. There were no differences in cell cycle and apoptosis between the control and MLN64 knockdown cells (data not shown).

To further evaluate the effect on adhesion by MLN64 knockdown in MDA-MB-231 cells, we adopted the Electric Cell Impedance Sensing (ECIS) method. As shown in Fig. 4C, the MDA-MB-231 Δ MLN64 cells showed a dramatically increased adhesion when compared with the control cells, as shown by a rapid rise in impedance, thus indicating stronger attachment ability to the electrode. The impedance of MDA-MB-231 Δ MLN64 cells at 160 min after seeding was 298 ± 30 ohms which was significantly higher than that of MDA-MB-231^{WT} (114 ± 25 ohms) and MDA-MB-231^{pEF} cells (137 ± 29 ohms), $p < 0.01$ for both comparisons (Fig. 4D).

From the adhesion assay *in vitro* and the ECIS assay, we found that suppression of MLN64 expression made the adhesion ability stronger in MDA-MB-231 cells. We further assessed downstream events following cell adhesion to the matrix surface by staining for 2 matrix adhesion regulatory molecules, paxillin and FAK. Staining for FAK in MDA-MB-231 Δ MLN64 cells was dramatically enhanced at focal adhesion sites (Fig. 5A). Interestingly, there was no difference

in the staining for paxillin in three sublines of MDA-MB-231 cells. Interestingly, in MCF-7 cells, there were rather strong staining signals for both FAK and paxillin at focal adhesion sites. FAK staining in MCF-7 Δ MLN64 cells had a little weaker signal compared to the MCF-7^{WT} and MCF-7^{pEF} cells (Fig. 5A). Using Western blot analysis, a significantly higher protein expression was seen in the MDA-MB-231 Δ MLN64 cells compared to both control cells (Fig. 5B).

A FAK inhibitor was then employed to assure the involvement of FAK in the regulation of adhesion by MLN64 in MDA-MB-231 cells. The FAK inhibitor (10 nM) diminished the effect of MLN64 knockdown on cell-matrix adhesion in MDA-MB-231 cells. When there was no FAK inhibitor added, MDA-MB-231 Δ MLN64 cells still had a significant increase (118.0 ± 10.9) in adhesion compared with both wild-type (78.9 ± 11.1) and plasmid control (89.5 ± 8.8). In exposure to FAK inhibitor (10 nM), the number of adherent cells was reduced to 68 ± 12.6 for MDA-MB-231 Δ MLN64 cells which was down to a similar level of both MDA-MB-231^{WT} (60.9 ± 19.0) and MDA-MB-231^{pEF} (60.4 ± 11.8) controls (Fig. 6).

Discussion

MLN64, reported first by Tomasetto *et al* (2), appears to be involved in cholesterol homeostasis and steroidogenesis (4,9,10,26-28). Moreover, it is suggested that MLN64 was overexpressed in some invasive breast cancers (14%), and breast cancer metastases (43%) (4). Immunoblot analysis from the same authors has shown that that expression of

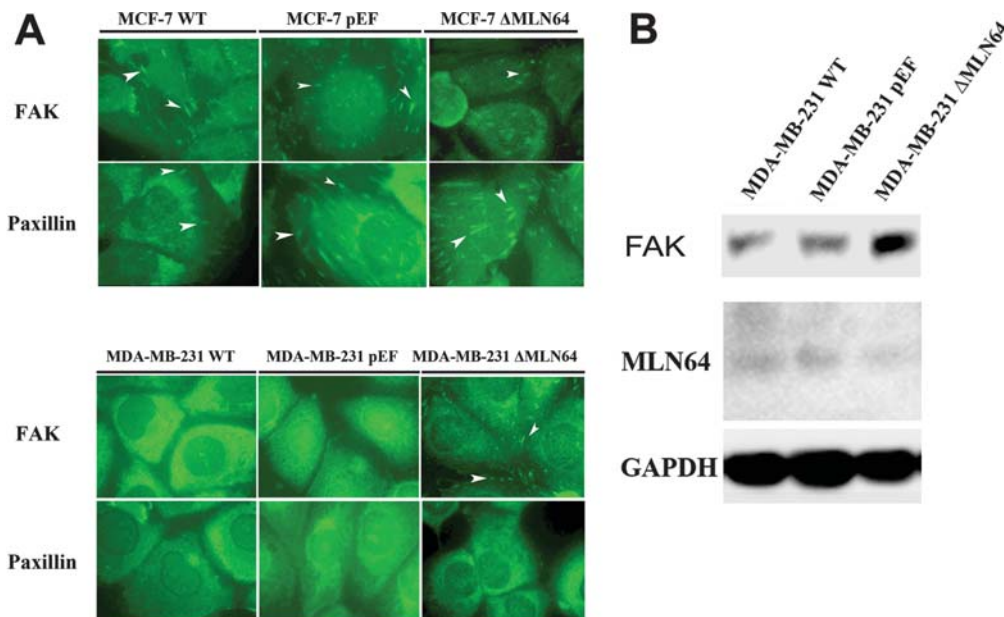


Figure 5. Effect on adhesion regulatory molecules by knockdown of MLN64. (A) Immunofluorescent staining of FAK and paxillin, which are indicated by arrows. Dramatically enhanced staining of FAK was seen in MDA-MB-231^{ΔMLN64} cells compared to MDA-MB-231^{WT} and MDA-MB-231^{pEF} cells. (B) Western blot analysis of FAK. MDA-MB-231^{ΔMLN64} cells showed a significantly elevated protein expression of FAK compare with both controls (top bands). A reduced protein level of MLN64 was also confirmed in MDA-MB-231^{ΔMLN64} cells compared to the controls using the Western blotting (the bands in the middle).

MLN64 protein exists in most breast cancer cell lines and breast cancer tissues, as well as in an ovary carcinoma cell line. The present study has also shown a dramatically stronger staining of MLN64 seen in breast cancer specimens compared to normal breast tissues and the presence of MLN64 in breast cancer cell lines.

MLN64 is frequently coamplified and expressed with *ERBB2* oncogene (2) and has been reported to correlate with breast patient prognosis. High expression of MLN64 correlated significantly with a short overall survival (OS) and disease-free survival (DFS). MLN64 is thus considered as a useful predictor for breast cancer (13). In the prostate cancer MLN64 expression seems to be correlated with high stage, high Gleason score and short relapse-free time in the prostate cancer patients (12). In the current study, the levels of MLN64 transcript in a breast cancer cohort were analysed against the corresponding clinical and pathological data. The result showed that patients with higher TNM staging or poor clinical outcome (with metastasis, local recurrence and died of breast cancer) had a relatively higher level of MLN64 expression. Moreover, the patients with higher MLN64 expression had a lower overall survival comparing to those with lower expression. Collectively, these clinical findings lead to a hypothesis that autonomous steroidogenesis can be present in the neoplastic tissue and that MLN64 may be implicated in an intratumoral steroidogenic process resulting in cancer progression (4).

Biological function of MLN64, especially its role in breast cancer, is far from clear. Our present study has revealed diverse roles played by MLN64 in breast cancer cells. Knockdown of MLN64 in MCF-7 cells lead to a reduction of *in vitro* cell growth, but this effect was not seen in the MDA-MB-231 cells. A recent study also demonstrated a positive role of MLN64 on proliferation of breast cancer cells

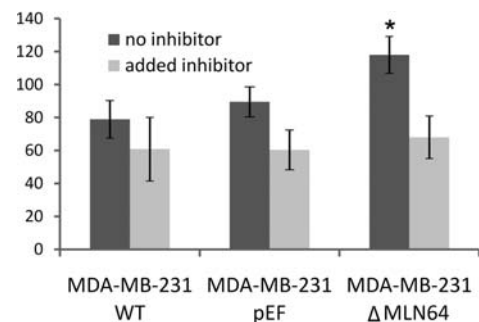


Figure 6. FAK inhibitor impaired the effect of cell adhesion by MLN64 knockdown in MDA-MB-231 cells.

(SKBR3 and BT474) (1). It suggests MLN64 can promote the cell proliferation thus contributing to the tumour growth at both primary and secondary sites. We examined the effect of MLN64 knockdown on cell cycle using a flow cytometry method. There was no obvious change seen in the cell cycle.

The most interesting observation from *in vitro* function assays was the alteration on cell-matrix adhesion by MDA-MB-231^{ΔMLN64} cells. The MDA-MB-231 cells became more adhesive when their MLN64 expression was suppressed by the ribozyme transgenes. This effect was seen in MDA-MB-231 cells using both cell-matrix adhesion assay and ECIS assay, but not in MCF-7 cells. Cell adhesion to extracellular matrix is predominantly regulated by the integrin signalling system. FAK is non-receptor tyrosine protein kinase localizing in cytoplasm that can be activated by integrin-ligand complex. FAK and paxillin can bind the transmembrane-integrin and cytoskeleton proteins, resulting in the connection of extracellular matrix and cytoskeleton to produce cell adhesion. It was reported that increased levels of

FAK were found in 85% (17 of 20) invasive tumours, and in 100% (all 15) metastatic tumours, suggesting that FAK overexpression may accompany changes in signal pathways involved in tumour cell invasion and metastasis (29). To elucidate the mechanism of the effect on adhesion, we examined two key molecules involved in the cell-matrix adhesion, focal adhesion kinase (FAK) and paxillin. The immunofluorescent staining showed a dramatically strong FAK staining in MLN64 knockdown cells while there was no signal exhibited by the wild-type and pEF-control cells. Western blot analysis also revealed an increase in the level of FAK protein in the MDA-MB-231^{ΔMLN64} compared to both controls. The effect on FAK was not seen in MCF-7 cells in which stronger staining of both FAK and paxillin was exhibited. This is consistent with the observations from cell-matrix adhesion assays and indicates that MLN64 may participate in the regulation of cell-matrix adhesion in MDA-MB-231 cells via FAK. This notion is supported by the experiments using a FAK inhibitor which diminished the effect of MLN64 knockdown on cell adhesion in MDA-MB-231 cells.

In conclusion, MLN64 is overexpressed in breast cancer. Higher expression level of MLN64 is correlated with poor prognosis and overall survival. Moreover, MLN64 can reduce the ability of adhesion of MDA-MB-231 cells and promote the growth in MCF-7 cell lines. We have further provided evidence to show that expression of MLN64 enabled the breast cancer cells to impair the cell-matrix adhesion via regulating the intergin-mediating FAK signalling pathway.

Acknowledgements

Dr W. Cai is a recipient of Cardiff University China Medical Scholarship. We wish to thank the Albert Hung Foundation and Cancer Research Wales for supporting our study.

References

- Kao J and Pollack JR: RNA interference-based functional dissection of the 17q12 amplicon in breast cancer reveals contribution of coamplified genes. *Genes Chromosomes Cancer* 45: 761-769, 2006.
- Tomasetto C, Regnier C, Moog-Lutz C, *et al.*: Identification of four novel human genes amplified and overexpressed in breast carcinoma and localized to the q11-q21.3 region of chromosome 17. *Genomics* 28: 367-376, 1995.
- Alpy F, Latchumanan VK, Kedinger V, *et al.*: Functional characterization of the MENTAL domain. *J Biol Chem* 280: 17945-17952, 2005.
- Moog-Lutz C, Tomasetto C, Regnier CH, *et al.*: MLN64 exhibits homology with the steroidogenic acute regulatory protein (STAR) and is over-expressed in human breast carcinomas. *Int J Cancer* 71: 183-191, 1997.
- Stocco DM: StAR protein and the regulation of steroid hormone biosynthesis. *Annu Rev Physiol* 63: 193-213, 2001.
- Tsujishita Y and Hurley JH: Structure and lipid transport mechanism of a StAR-related domain. *Nat Struct Biol* 7: 408-414, 2000.
- Kusakabe M, Todo T, McQuillan HJ, Goetz FW and Young G: Characterization and expression of steroidogenic acute regulatory protein and MLN64 cDNAs in trout. *Endocrinology* 143: 2062-2070, 2002.
- Mathieu AP, Fleury A, Ducharme L, Lavigne P and LeHoux JG: Insights into steroidogenic acute regulatory protein (StAR)-dependent cholesterol transfer in mitochondria: evidence from molecular modeling and structure-based thermodynamics supporting the existence of partially unfolded states of StAR. *J Mol Endocrinol* 29: 327-345, 2002.
- Alpy F, Stoeckel ME, Dierich A, *et al.*: The steroidogenic acute regulatory protein homolog MLN64, a late endosomal cholesterol-binding protein. *J Biol Chem* 276: 4261-4269, 2001.
- Watari H, Arakane F, Moog-Lutz C, *et al.*: MLN64 contains a domain with homology to the steroidogenic acute regulatory protein (StAR) that stimulates steroidogenesis. *Proc Natl Acad Sci USA* 94: 8462-8467, 1997.
- Maqani N, Belkhir A, Moskaluk C, Knuutila S, Dar AA and El-Rifai W: Molecular dissection of 17q12 amplicon in upper gastrointestinal adenocarcinomas. *Mol Cancer Res* 4: 449-455, 2006.
- Stigliano A, Gandini O, Cerquetti L, *et al.*: Increased metastatic lymph node 64 and CYP17 expression are associated with high stage prostate cancer. *J Endocrinol* 194: 55-61, 2007.
- Vinatzer U, Dampier B, Streubel B, *et al.*: Expression of HER2 and the coamplified genes GRB7 and MLN64 in human breast cancer: quantitative real-time reverse transcription-PCR as a diagnostic alternative to immunohistochemistry and fluorescence in situ hybridization. *Clin Cancer Res* 11: 8348-8357, 2005.
- Bieche I, Tomasetto C, Regnier CH, Moog-Lutz C, Rio MC and Lidereau R: Two distinct amplified regions at 17q11-q21 involved in human primary breast cancer. *Cancer Res* 56: 3886-3890, 1996.
- Kauraniemi P, Barlund M, Monni O and Kallioniemi A: New amplified and highly expressed genes discovered in the ERBB2 amplicon in breast cancer by cDNA microarrays. *Cancer Res* 61: 8235-8240, 2001.
- Jiang WG, Watkins G, Fodstad O, Douglas-Jones A, Mokbel K and Mansel RE: Differential expression of the CCN family members Cyr61, CTGF and Nov in human breast cancer. *Endocr Relat Cancer* 11: 781-791, 2004.
- Zuker M: Mfold web server for nucleic acid folding and hybridization prediction. *Nucleic Acids Res* 31: 3406-3415, 2003.
- Jiang WG, Davies G, Martin TA, *et al.*: Targeting matrilysin and its impact on tumor growth in vivo: the potential implications in breast cancer therapy. *Clin Cancer Res* 11: 6012-6019, 2005.
- Ye L, Kynaston H and Jiang WG: Bone morphogenetic protein-9 induces apoptosis in prostate cancer cells, the role of prostate apoptosis response-4. *Mol Cancer Res* 6: 1594-1606, 2008.
- Jiang WG, Hiscox S, Hallett MB, Horrobin DF, Mansel RE and Puntis MC: Regulation of the expression of E-cadherin on human cancer cells by gamma-linolenic acid (GLA). *Cancer Res* 55: 5043-5048, 1995.
- Jiang WG, Hiscox SE, Parr C, *et al.*: Antagonistic effect of NK4, a novel hepatocyte growth factor variant, on in vitro angiogenesis of human vascular endothelial cells. *Clin Cancer Res* 5: 3695-3703, 1999.
- Giaever I and Keese CR: Micromotion of mammalian cells measured electrically. *Proc Natl Acad Sci USA* 88: 7896-7900, 1991.
- Keese CR, Wegener J, Walker SR and Giaever I: Electrical wound-healing assay for cells in vitro. *Proc Natl Acad Sci USA* 101: 1554-1559, 2004.
- Jiang WG, Ablin RJ, Kynaston HG and Mason MD: The prostate transglutaminase (TGase-4, TGaseP) regulates the interaction of prostate cancer and vascular endothelial cells, a potential role for the ROCK pathway. *Microvasc Res* 77: 150-157, 2009.
- Jiang WG, Grimshaw D, Lane J, *et al.*: A hammerhead ribozyme suppresses expression of hepatocyte growth factor/scatter factor receptor c-MET and reduces migration and invasiveness of breast cancer cells. *Clin Cancer Res* 7: 2555-2562, 2001.
- Bose HS, Baldwin MA and Miller WL: Evidence that StAR and MLN64 act on the outer mitochondrial membrane as molten globules. *Endocr Res* 26: 629-637, 2000.
- King SR, Ginsberg SD, Ishii T, Smith RG, Parker KL and Lamb DJ: The steroidogenic acute regulatory protein is expressed in steroidogenic cells of the day-old brain. *Endocrinology* 145: 4775-4780, 2004.
- Tuckey RC, Bose HS, Czerwionka I and Miller WL: Molten globule structure and steroidogenic activity of N-218 MLN64 in human placental mitochondria. *Endocrinology* 145: 1700-1707, 2004.
- Weiner TM, Liu ET, Craven RJ and Cance WG: Expression of focal adhesion kinase gene and invasive cancer. *Lancet* 342: 1024-1025, 1993.